N-63-4-3

FACETING OF COPPER SURFACES AT 1000°C†

by

W. M. Robertson††

† This paper is based on a thesis submitted in partial fulfillment of the requirements for the Doctor of Philosophy Degree at Carnegie Institute of Technology, Pittsburgh, Pa.

†† Presently at the Metallurgy Department, The University, Leeds, England; formerly NSF Graduate Fellow at Carnegie Institute of Technology.

FACETING OF COPPER SURFACES AT 1000°C

by W. M. Robertson

Abstract

Polished copper surfaces were observed to facet on annealing at 1000°C in wet hydrogen atmospheres. It was found that the quantity $\ell n\ p_{H_2O}/p_{H_2}$ must be greater than zero for extensive faceting to occur, though some faceting particularly at the facet edges, can occur for $\ell n\ p_{H_2O}/p_{H_2}$ as small as -3.5. The criteria for faceting to occur by the reduction of surface free energy are discussed and it is shown that facets near the (111) orientation are thermodynamically stable. The effect of anisotropy of surface free energy on facet nucleation is discussed.

The outlines of lens-shaped facets were measured. The shapes and sizes of the lens-shaped facets are consistent with a volume diffusion mechanism of facet formation. The observed profiles of the curved surfaces near separated linear facets are compared to theoretically calculated profiles. The calculations by Mullins of facet profiles are extended slightly to facilitate the comparison. The observed profiles are in reasonable agreement with the calculated profiles for facet formation by surface diffusion with the surface diffusion coefficient the same on both the low index and the complex surfaces.

Introduction

The thermal faceting of metal surfaces has been observed under a variety of experimental conditions. Some rather important questions concerning this phenomenon, however, remain unanswered.

One point of controversy has been the question of the driving force for facet formation. Is a faceted surface a minimum energy, equilibrium structure? Or do facets form only when a kinetic process of net evaporation is occurring at the surface? Recently, Moore[1] has critically reviewed the evidence on this question and indicates that evaporation is quite important if not the most important cause. Evidence is presented in the present work which indicates that the driving force for facet formation is the reduction of surface free energy in the system, so that under the observed conditions facets are equilibrium structures.

A second point of uncertainty concerns the mechanism by which facets form, assuming that a completely faceted surface is the equilibrium structure. There are several possibilities for the mechanism: surface diffusion; volume diffusion within the crystal; diffusion of the vapor in an ambient gaseous atmosphere; and evaporation from the surface. Mullins[2] has analyzed the growth of facets by these various mechanisms. His analysis offers possibilities for distinguishing which of the mechanisms is predominant under given experimental conditions. In the present paper these calculations are extended slightly, and evidence is presented which indicates that under the conditions of these experiments volume diffusion is the predominant mechanism of the formation of separated facets. It is

observed, however, that the facet shapes are quite similar to the shapes predicted by Mullins for the surface diffusion mechanism.

Experimental Procedure

The experimental method was to polish surfaces on copper samples, anneal them in a wet hydrogen atmosphere and measure facet shapes from interference photomicrographs of the faceted surfaces.

The material used was 99.999% pure copper from the American Smelting and Refining Company. Many of the samples were sections of symmetric tilt bicrystals, grown in high purity graphite in vacuum as described by Mullins and Shewmon[3]. The use of bicrystals is, of course, not essential to the experiments; the bicrystals had been produced to measure torques on the surfaces and provided surfaces of known orientation on which to observe facets. The remainder of the samples were large-grained polycrystals of the same copper. After melting and solidifying in a high purity graphite mold in vacuum, the bar was reduced in thickness by twenty percent by cold rolling, and annealed in dry pure hydrogen at 1050°C for twenty hours. (Attempts to grow large grains in the AS&R copper without first vacuum melting were always unsuccessful.) The grains were oriented optically[4], then repolished through Microcut polishing paper, and finally electropolished[3].

The samples were annealed in a quartz tube inside a Nichrome wound furnace for twenty to forty hours at 1000°C $\pm$ 5°C. The results did not vary appreciably with the time of annealing when the time was long enough to allow the facets to form extensively (longer than about four

hours). The samples were set in a high purity alumina boat and covered with a loose-fitting cover made of 99.99% pure copper foil. The sample temperature was measured by a Chromel-Alumel thermocouple placed next to the copper cover. To provide the annealing atmosphere, a prepurified mixture of 1% hydrogen, 99% nitrogen from Matheson Chemical Company was passed through a Deoxo unit and then either (a) through a magnesium perchlorate-Drierite drying column (dew point = -50°C) or (b) directly into the furnace (dew point = -20°C), or (c) through distilled water cooled by an ice bath (dew point = 0°C) or (d) through room temperature distilled water (dew point = 25°C). Some runs were made with commercial, pure hydrogen with the dew point controlled as in (a)-(d) above. The dew point was measured as the gas flowed out of the quartz tube at a flow rate of about one-half cubic foot per hour.

The annealed surfaces were observed and photographed with a Zeiss interference microscope and measurements were made on the enlarged micrographs.

Results

The results will be presented in four sections. In the first section the experimental conditions of atmosphere and surface orientation under which facets were observed are described. In the second section the conditions on the anisotropy of surface energy for facets to be stable are discussed and compared with the anisotropy measured in earlier work[5,6]. In the third section measurements of the shapes of lenticular facets are described and from these measurements evidence about the mechanism of facet

formation is deduced. In the final section Mullins'[2] calculations on the kinetics of facet formation are extended slightly and the predicted profiles of the curved surfaces near facets are compared with the experimentally observed profiles.

1. Experimental Conditions for Faceting

To obtain extensive faceting on oxygen free copper it was found that the ratio p_{H_2O}/p_{H_2} must be greater than about one. A ratio this high is difficult to obtain by adding water to pure hydrogen, since it requires a dew point that is well above room temperature. It is therefore not surprising that Bénard et al.[7] did not observe faceting in water/hydrogen mixtures, since they started with pure hydrogen. However, a water/hydrogen ratio greater than one is readily obtained by adding water to a nitrogen-1% hydrogen mixture.

No faceting at all was observed for $\ell n\ p_{H_2O}/p_{H_2}$ less than -3.5. Facets were observed for some orientations for $\ell n\ p_{H_2O}/p_{H_2} = -3.5$. Figure 1 shows the orientations that faceted. For this water/hydrogen ratio the extent of faceting was quite variable over the sample surfaces. The grains of which the orientations are plotted in Figure 1 were near the sample edges; away from the sample edges practically no faceting occurred. The unfaceted orientations of Figure 1 were edge grains immediately adjacent to heavily faceted grains, so that the orientation was the only factor affecting whether or not faceting occurred. Similar distributions of faceting were observed by Moore[8] and by Moreau and Bénard[9].

A possible explanation for the difference between the edges and centers of the specimens is that nucleation of facets may have been easier

at the sample edges than in the sample centers. However, the individual facets did not appear to be directly connected to the sample edge. The nucleation of facets will be discussed further in the next section.

For $\ell n\ p_{H_2O}/p_{H_2} \geq 0$, all orientations were observed to facet. For surfaces near (100) and (111) the entire surface broke up into fine facets after an anneal of a few hours. For orientations fairly far removed from (100) and (111) the facets were larger and more separated. This difference is associated with the ease of nucleation of facets as a function of orientation. Near (100) and (111) nucleation is easy and many small facets can form; further away nucleation is more difficult and only a few facets will nucleate, each one then growing fairly large.

In every case the faceted surface consists of flat sections of low index plane connected by more or less curved surfaces of high index. In nearly every case the low index plane was (100) or (111); very rarely a small area of (110) plane would appear, when the original surface was close to (110). For some orientations both (100) and (111) facets would appear on the same surface. Figure 2 shows this on a surface about 20° from (100) lying on the great circle between (100) and (111). It can be seen that the facet surfaces are very steeply inclined to the original surface.

The extent of faceting on one grain sometimes seemed to affect the extent of faceting on a neighboring grain. When a highly faceted grain abutted a lightly faceted one, there very often was a facet free zone on the lightly faceted grain near the grain boundary, as illustrated in Figure 3. An explanation has not been found for this phenomenon. It is

interesting to note that Dunn and Walter[10] found a similar effect in the oxidation of silicon iron. They showed that it was due to grain boundary motion. No evidence that boundary migration had occurred was found, however, in the present case.

2. Driving Force for Facet Formation

There has been some controversy as to the driving force for facet formation. Chalmers, King and Shuttleworth[11] proposed that the energy of the system could be lowered by an initially flat surface breaking up into facets of two or more other orientations, at least one of which had considerably lower surface free energy, γ, than the original surface. Several later workers have explained their results on this basis, particularly Bénard and co-workers[7,9,12-16] and Rhead and Mykura[17,18,19]. However, Hondros and Moore[2,20,21] found that net evaporation of metal from the surface appeared to be a necessary condition for facet formation on silver. They proposed that the facets formed due to the kinetics of evaporation and were not due to a minimization of surface free energy.

The conditions on the anisotropy of surface free energy for facets to be stable will now be examined. The variation of surface free energy with orientation is usually represented by the "γ-plot", in which the surface free energy of a surface with normal $\underline{n}$ is represented as a vector parallel to $\underline{n}$ of length proportional to γ. The γ-plot for a crystal is a three-dimensional closed surface with at least the symmetry of the crystal structure. Following Herring[22,23], consider a sphere passing through the origin of the γ-plot which is tangent to the γ-plot at a given orientation. If the tangent sphere lies everywhere inside the γ-plot except

at the tangent point, a smooth surface of the given orientation will be stable with respect to a faceted surface. If, however, the γ-plot passes inside the tangent sphere at any point, then a faceted surface will be more stable than the original smooth surface.

If the curvature of the γ-plot at the orientation being considered is greater than the curvature of the tangent circle, then the γ-plot will pass inside the circle in the vicinity of the point of tangency and a faceted surface will be stable. Gruber[24] has shown that this case corresponds to the condition

$$\gamma + \frac{\partial^2 \gamma}{\partial \theta^2} < 0 \qquad (1)$$

for stable facets. If the inequality is reversed, then a flat surface is stable.

The derivative of surface free energy with respect to orientation, $(\partial \gamma / \partial \theta) \equiv \tau$, was called a "torque term" by Herring[25]. Mykura[26,27] has shown that the quantity τ/γ can be measured as a function of orientation. Gjostein[28] has shown that relation (1) is equivalent to the condition that the magnitude of the slope of a plot of τ/γ versus θ should be greater than unity, i.e., $\left|\frac{\partial}{\partial \theta} (\tau/\gamma)\right| > 1$. The present authors measured τ/γ as a function of orientation on copper surfaces which were also faceting[5]. Figure 4 shows a plot of τ/γ versus θ for surfaces near (111) along the great circle between (111) and (100) for conditions of extensive faceting. It can be seen that for θ near zero the magnitude of the slope of the curve is greater than unity. Thus facets in this range of orientations are indeed thermodynamically stable. Figure 5, from an earlier work[6],

shows that stable facets would not be expected in a dry hydrogen atmosphere; they were never observed under these conditions. It should be pointed out however, that facets were observed near (100) under the conditions of Figure 4, when the τ/γ vs θ curve would not indicate facets to be stable[5]; similarly, the τ/γ vs θ plot would not indicate stable facets at either (100) or (111) under the conditions of Figure 1. These observations indicate that for at least one case facets are stable; but also under some conditions facets may appear when they would not be expected due to anisotropy of surface free energy.

Torques can be measured from the angles at the edges of facets, assuming the facets are equilibrium structures. Figure 6, a section through a facet, defines the relevant angles. Two relations are of interest:

$$\frac{\partial \gamma_s}{\partial \theta} = \gamma_c \sin\theta + \frac{\partial \gamma_c}{\partial \theta} \cos\theta \qquad (2)$$

$$\gamma_s = \gamma_c \cos\theta - \frac{\partial \gamma_c}{\partial \theta} \sin\theta \, . \qquad (3)$$

These relations are readily derived from Herring's relations[25] for the intersection of three interfaces by setting the energy and torque on one interface equal to zero. They were used by Mykura[27] to estimate torques from facets on nickel. When θ is of the order of fifteen degrees or more, as is commonly observed for facets, then $\partial\gamma/\partial\theta$ is usually quite small, so that relations (2) and (3) are approximated by

$$\frac{\partial \gamma_s}{\partial \theta} = \gamma_c \sin\theta \, , \qquad (2a)$$

$$\gamma_s = \gamma_c \cos\theta \ , \qquad (3a)$$

giving

$$\frac{1}{\gamma_s} \frac{\partial \gamma_s}{\partial \theta} > \tan\theta \ . \qquad (2b)$$

Therefore tan θ gives a lower limit for the torque at the low index plane of a facet. This relation was used by Gjostein[29] to estimate torques on faceted surfaces. Similarly, cos θ is an estimate of the ratio of the surface free energies of the low index and high index facet surfaces. This relation was used by Moore[8]. In the present work relations (2b) and (3a) were used to estimate the torques and the ratios of surface free energies for a number of facets which had (111) as the low index plane. The results of these measurements are presented in Figure 7. There is considerable scatter in the results, but the average value of $\frac{1}{\gamma_s} \frac{\partial \gamma_s}{\partial \theta}$ is just slightly greater than the value at θ = 0 of Figure 4; hence Figures 4 and 7 are in reasonably good agreement with one another. No edge angles were measured for (100) facets because the small size of the (100) facets gave poorly defined interference fringe patterns at the facet edges.

The ratios of the surface free energies of (111) and high index surfaces as measured at facets using relation (3a) are in reasonable agreement with these ratios as determined by integration of the plot of τ/γ versus θ in Figure 4. Figure 4 gave $\gamma_{111}/\gamma_\theta = 0.960$[5], while the average value of γ_o/γ_θ for (111) from Figure 6a is 0.952.

A further point that will now be examined is the fact that facets were observed at angles of more than 0.15 radian from (111), where the slope of the τ/γ vs θ plot becomes less than unity. Relation (1) indicates

that in this region facets should not appear. However, relation (1) does not include all cases for which facets can be stable. It applies to orientations for which the curvature of the γ-plot is greater than that of the tangent sphere so that the γ-plot lies inside the tangent sphere infinitesimally close to the point of tangency. However, facets are also stable if the γ-plot curvature is less than that of the tangent sphere at the point of tangency, but penetrates the tangent sphere at a point a finite distance away from the point of tangency. The two cases are illustrated on two-dimensional sections of the γ-plot in Figure 8. The plot of τ/γ vs θ for Figure 8b would be similar to Figure 4.

It is of interest to be able to determine from Figure 4 the total range of orientations which should facet. To do this, consider Figure 9. The sphere tangent at B just touches the γ-plot at A. The angle θ' is the limiting angle for stable facets. For $\theta < \theta'$ the γ-plot pierces the tangent sphere near A as in Figure 8b and facets are stable; for $\theta > \theta'$ the sphere lies entirely inside the γ-plot and the surfaces will not facet. On a τ/γ vs θ plot, the sphere ADB gives a line of slope $1 (\theta << 1)$; the γ-plot ACB gives a curve similar to the solid curve of Figure 4. The sphere and the γ-plot are tangent at B; therefore the line of slope 1 and the τ/γ vs θ curve will cross at θ'. Also the γ-plot and the sphere coincide at points A and B; therefore $\int_{\theta=A}^{\theta=B} \frac{1}{\gamma} \frac{\partial \gamma}{\partial \theta} d\theta$ must be the same for both the γ-plot and the sphere. Therefore, to determine the limit of faceting, θ', given a τ/γ vs θ curve similar to Figure 4, draw a line of slope 1 on the curve such

that the area beneath the line of slope 1 equal the area beneath the given curve over the interval $\theta = 0$ to $\theta = \theta'$. Then θ' is the angle of the second crossing point of the two curves. This is illustrated in Figure 4; the dashed line has slope 1, and θ' is indicated. The value of θ' found is about 0.19 radian ($\simeq 11°$) so that orientations up to 0.19 radian from (111) should facet. Actually surfaces further than this from (111) were observed to facet. However, the solid curve of Figure 4 is only approximate, and θ' can vary considerably with small changes in the curve, so it is not surprising that the agreement is not exact.

The considerations of the preceding paragraph are relevant to the nucleation of facets. Mullins[2] has pointed out two cases: (a) when the γ-plot penetrates the tangent sphere in the vicinity of the tangent point, an initially flat surface can lower its energy breaking up into facets of orientations infinitesimally different from the original orientation so that no nucleation barrier exists; when the γ-plot lies outside the tangent sphere in the region of tangency but penetrates the sphere at a point further removed, a small area of facet of an orientation considerably different from the original orientation must be found, requiring the expenditure of a finite amount of free energy and presenting an activation barrier to facet formation. (In both cases there will also be a nucleation barrier arising from the extra energy of a facet edge. So far it has not been possible to estimate how strong a barrier this is.)

Orientations for which equation (1) holds fall in case (a) of the previous paragraph, and there is no nucleation barrier to facet formation. This corresponds to the region of Figure 4 for which the magnitude

of the slope is greater than unity. It was observed that orientations near (111) were completely covered with small facets, the behavior that would be expected if there were no nucleation barrier.

Orientations in Figure 4 for which the slope is less than unity, but with $\theta < \theta'$, fall in case (b). It was observed that for orientations about ten degrees or more from (111) the facets were very often large and widely separated from one another, the behavior that would be expected if a nucleation barrier existed. In studies of the kinetics of facet formation, to be described more fully in the next two sections, it is desirable to be able to observe large, separated facets. Therefore these studies will be most readily done on orientations for which the slope of the γ/θ plot is less than one, but for which $\theta < \theta'$. For copper in wet hydrogen these conditions are met in the range of about ten to twenty degrees from (111).

One final point regarding the stability of facets is of interest here. It was shown previously[30] on the basis of a step model of the surface that the surface free energy as a function of orientation near a cusp could be expressed as follows:

$$\gamma(\theta) = \gamma_s \cos\theta + f_1 \sin\theta + f_2 \theta^2 \qquad (4a)$$

$$= \gamma_s + f_1 \theta + (f_2 - \gamma_s)\theta^2, \ (\theta \ll 1), \qquad (4b)$$

where γ_s is the surface free energy per unit area at the cusp orientation, f_1 is a constant proportional to the free energy increase per unit length of step added, and f_2 is a constant proportional to the interaction energy

between single steps, i.e., the amount of free energy per unit length by which a double step differs from the two constituent single steps. When the total variation in γ is not large,

$$\frac{\tau}{\gamma} \simeq \frac{\tau}{\gamma_s} = \frac{f_1}{\gamma_s} + \left(\frac{2f_2}{\gamma_s} - 1\right)\theta. \qquad (5)$$

The slope of the τ/γ vs θ plotis given by the bracketed expression. If $f_2 < 0$ (attraction between steps), then $\left|\frac{1}{\gamma_s}\frac{\partial \tau}{\partial \theta}\right| > 1$, and facets are stable. If $f_2 > 0$ (repulsion between steps), then $\left|\frac{1}{\gamma_s}\frac{\partial \tau}{\partial \theta}\right| < 1$ and facets are unstable.

The same result can be obtained using the basic equation for the reduction of energy in faceting given by Moore[8]. If γ_u is the surface free energy of the original unfaceted surface and γ_f the average surface free energy of the faceted surface, then the condition for faceting to occur is

$$\gamma_u > \gamma_f = \frac{\gamma_s \sin\beta + \gamma_c \sin\alpha}{\sin(\alpha+\beta)} .$$

From equation (4a), $\gamma_s = \gamma(0)$ and $\gamma_c = \gamma(\alpha+\beta)$. Hence the condition for faceting reduces to

$$\gamma_u - \gamma_2 = f_2 \left[\alpha^2 - \frac{(\alpha+\beta)^2 \sin\alpha}{\sin(\alpha+\beta)}\right]$$

$$\simeq f_2(-\alpha\beta) \qquad (\sin(\alpha+\beta) \simeq \alpha+\beta)$$

being greater than or less than zero. Hence $\gamma_u - \gamma_f > 0$ for $f_2 < 0$

(attraction between steps) and $\gamma_u - \gamma_f < 0$ for $f_2 > 0$ (repulsion between steps).

Thus, the criteria for faceting find complete agreement in the step model of the surface; if steps attract one another, they tend to bunch up and faceting occurs; if steps repel one another, facets are unstable with respect to a smooth surface. It would be desirable to be able to explain the attraction or repulsion of steps on an atomistic basis; however, this has not yet been possible.

3. Mechanism of Facet Formation

In the previous section it was deduced that under the conditions of these experiments the driving force for facet formation is the minimization of surface free energy. In this section measurements are described of the shapes of separated, lens-shaped facets. These shapes give information on the mechanism of facet formation.

Mullins[2] calculated the kinetics of widening of linear facets, under the driving force of a minimization of surface free energy in the system. He showed that the width of a facet is proportional to the p^{th} root of the time since the facet started growing; p is 2 for formation by evaporation-condensation of the metal in contact with its own dilute vapor; p is 3 for evaporation-condensation in the presence of a surrounding gas, where diffusion of the metal vapor in the gas limits the rate of material transport; p is also 3 for formation by volume diffusion in the crystal; p is 4 for facet formation by surface diffusion on the metal. Mullins argued qualitatively that the tip of a lengthening facet will attain a constant velocity, so the length of the facet will be proportional

to the first power of the time. Therefore "the width of the facet at a given point should be proportional to the p^{th} root of its distance from the facet tip that originally swept by the point"[2], where p has one of the values given above.

It was noted earlier that separated linear facets were obtained on surfaces ten to twenty degrees from (111). Typical facets of this type are shown in Figure 10. The widths of such facets were measured as a function of the distance from the facet end. Figure 11 is a typical logarithmic plot of facet width, w, versus distance from the facet end, ℓ. The dashed line, a least squares line based on all the points, has a slope of 0.394. Since $w \propto \ell^{1/p}$, the slope of this plot should equal 1/p. Figure 12 shows the frequency of occurrence of various values of the slopes of such logarithmic plots. The average of 25 slopes is 0.422.

Before drawing conclusions about the value of 1/p from the above data, an approximate calculation will be made to determine how accurately the facet shape reflects the mechanism of formation. Near the end of a facet, the facet sides are not parallel, but come together. The curvature of the complex curved surfaces increases near the facet tip. This curvature gradient along the length of the facet drives a flux of material along the facet length. This flux could cause the facet shape to depart from the assumed relation, $w \propto \ell^{1/p}$. For the slope of the log w - log ℓ plot to have any significance, the flux along the facet length must be much less than the flux perpendicular to the facet length.

Assume that the radius of curvature R of the curved surface is the same as that of a circle tangent to the curved surface at the edge

of the facet (Point 0, Figure 6) and to the original surface. Then[2]

$$R = \frac{n\,w}{2m^2}$$

where $n = -\tan\alpha$ $(n > 0)$, and $m = \tan\beta$. The material on the curved surface has an excess chemical potential, $\Delta\mu$, due to the curvature of the surface: $\Delta\mu = \gamma/R$. The flux J_w tending to widen the facet is

$$J_w \simeq \frac{2D\,\Delta\mu}{kT(w + 2Rm)} = \frac{4D\,\gamma}{kT(n/m^2)(1 + n/m)w^2} ,$$

where the appropriate diffusion coefficient D depends on the mechanism of facet formation.

The flux J_ℓ along the length of the facet has the order of magnitude

$$J_\ell = \frac{-D}{kT}\,\frac{d(\Delta\mu)}{d\ell} = \frac{-2D\gamma}{kT(n/m^2)}\,\frac{d}{d\ell}\left(\frac{1}{w}\right) .$$

It is assumed that

$$w = a\,\ell^{1/p}$$

where a is a proportionality constant, and w and ℓ are measured in the same units. So

$$\frac{d}{d\ell}\left(\frac{1}{w}\right) = \frac{-1}{ap\,\ell^{1/p+1}} = \frac{-a^p}{pw^{1+p}} ,$$

$$J_\ell = \frac{2D\gamma\,a^p}{kT(n/m^2)p\,w^{1+p}} .$$

The quantity of interest is the ratio of the two fluxes above:

$$r = \frac{J_\ell}{J_w} = \frac{a^p(1 + n/m)}{2p\, w^{p-1}} = \frac{w}{2\ell} \frac{(1 + n/m)}{p} .$$

The ratio r should be small if the facet is to widen strictly as $t^{1/p}$; take as an appropriate value $r \leq 0.1$. Then the condition for the slope of the log w - log ℓ plot to be significant is

$$\frac{w}{\ell} \leq \frac{2(0.1)\ p}{(1 + n/m)} . \qquad (6)$$

For all of the facets measured, n/m = 1. For Figure 11, p = 1/0.394 = 2.5.

So the slope of the portion of the curve for $w \geq 0.25\ell$(small w and ℓ) is not significant; this point is marked by the arrow in Figure 11. For nearly all the facets measured, the minimum value of ℓ which satisfies condition (6) lies between four and five millimeters at the magnification used. Since the facet width was measurable for at least 30 mm along each facet, only the first few points are affected by the flux along the facet length.

The above calculation indicates that the slope of the log w - log ℓ plot is significant in the elucidation of the mechanism of facet formation. To eliminate the contribution to widening due to the flux along the facet length, the slopes were recalculated, neglecting the points for $\ell < 5$ mm. The solid line of Figure 11 is a least squares line based on the points for $\ell \geq 5$ mm. The recalculated slopes are shown in

Figure 13. It can be seen that the recalculated values are more closely grouped than the original values; the standard deviation σ has decreased from 0.087 to 0.064 for the twenty-five values. The final value of 1/p, 0.361, is quite close to 1/3; thus the mechanism of facet formation appears to be mainly volume diffusion in the crystal and/or diffusion in the surrounding atmosphere.

Mullins[2] discussed the ranges of facet widths for which the various transport mechanisms would be dominant. Surface diffusion would be expected to predominate for very narrow facets, particularly near the tip of an extending facet. Since the above calculation indicates that near the tip the relation $w = a\,\ell^{1/p}$ should not be applicable because of the flux along the facet length, it appears that facets growing by surface diffusion will be difficult to observe.

A value of 1/p near 1/3 is consistent with facet formation by diffusion in the surrounding gas. However, Mullins indicated[2] that, for gaseous diffusion to predominate, the vapor pressure of the crystal should be greater than $\sim 10^{2}$ dynes/cm^{2}. The measured vapor pressure of pure copper at 1000°C is $\sim 10^{-2}$ dynes/cm^{2} [31]. The presence of oxygen in the atmosphere could conceivably cause the effective vapor pressure of copper to be appreciably higher than in vacuum, but it seems unlikely that the pressure would be increased by the factor of 10^{4} necessary to explain the present results. Hence, it can be concluded that gaseous diffusion is unimportant in the present case.

The alternative explanation for 1/p near 1/3 is volume diffusion in the crystal. Under the conditions of these experiments, volume diffusion

will be expected to predominate over surface diffusion for facets wider than about five microns. This was the approximate width of the observed facets, so the experimental results are consistent with facet formation by volume diffusion in the crystal. It should be noted, however, that several experimental studies of copper[3,32-34] and silver[19] have shown that surface diffusion is the predominant transport mechanism for the growth of grain boundary grooves up to widths of ten microns and more. Of course, the width for a facet which is comparable to a grain boundary groove is not just the facet width but includes also the curved surfaces adjacent to the facet, a total width in the present case of 15-20 microns.

In conclusion of this section, it appears that the predominant mechanism for facet formation under the conditions of these experiments is volume diffusion in the crystal.

4. Profiles of Curved Surfaces of Facets

Interference micrographs of separated facets such as Figure 10 show the profile of the curved surface near the facet. In this section the observed profiles are compared with those calculated by Mullins[2], and, to facilitate the comparison, Mullins' calculations are extended slightly.

Mullins considered facet formation by three mechanisms: (a) evaporation and condensation of the metal in contact with its dilute vapor; (b) evaporation and condensation of the metal in contact with a surrounding fluid, where diffusion of metal vapor in the fluid limits the rate of material flow - the same treatment also covers volume diffusion in the crystal; and (c) surface diffusion. For (a) and (c), he derived

the shapes of the curved profiles and relations describing the kinetics of formation. Case (b) was too complex to treat exactly so he derived approximate relations describing the growth kinetics.

The observed profiles always showed a maximum (or minimum) somewhat away from the intersection of the curved and flat surfaces. A maximum like this is one of the features exhibited by the calculated profiles for facet formation by surface diffusion (Figure 14). A similar maximum might be expected for growth by volume diffusion in the crystal or vapor, in analogy with the case for grain boundary grooving by volume diffusion[35] which forms a profile very similar to that developed by surface diffusion. The existence of this maximum implies that mechanisms (b) and/or (c) predominate, since the calculated profile for case (a) does not show a maximum. The considerations of the preceding sections indicate that volume diffusion is the dominant mechanism. Nevertheless, it is still of some interest to compare the observed profiles with those predicted for the surface diffusion mechanisms.

An observed (or calculated) profile at a given time is a plot of y, the distance of the surface from the original flat surface, as a function of x, the distance from the middle of the facet. A given profile has a constant shape which expands uniformly with time, t. The physical parameters of the system on which the exact shape depends are as follows: $m = \tan \beta$ and $n = -\tan \alpha$ (see Figure 6); $B = D_c \Omega^2 \nu \gamma_c / kT$, where D_c is the surface diffusion coefficient on the curved surface, Ω the atomic volume of the crystal atoms, ν the number of atoms per cm^2 that participate in the diffusion, γ_c the surface free energy of the curved surface

and kT has its usual meaning; $(D_s/D_c)\cos\alpha \equiv d\cos\alpha$ where D_s is the surface diffusion coefficient on the simple plane. The exact form of y is

$$y(x,t) = m\,(Bt)^{1/4}\,Z\left[\frac{x}{(Bt)^{1/4}}\right], \qquad (7)$$

where $Z(u) = C_3Z_3(u) + C_4Z_4(u)$.

The quantities C_3 and C_4 are constants which depend on m, n and d, while $Z_3(u)$ and $Z_4(u)$ are functions satisfying the differential equation and boundary conditions for the system. To calculate C_3 and C_4, Mullins introduced a parameter ω which describes the rate at which the facet widens and deepens:

$$x^{\blacktriangle} = \omega\,(Bt)^{1/4}$$

$$y^{\blacktriangle} = -\,n\,\omega(Bt)^{1/4}$$

where $x^{\blacktriangle}$ and $y^{\blacktriangle}$ are the coordinates of the point of intersection of the flat and curved surfaces on the facet profile. Mullins derived relations from which C_3, C_4 and ω could be calculated, and calculated these quantities for the two limiting cases $d\cos\alpha = 0$ (zero diffusion coefficient on the flat) and $d\cos\alpha = \infty$ (infinite diffusion coefficient on the flat). Mullins tabulated values[36] of Z_3 and Z_4 and their derivatives for comparison calculations for intermediate values of $d\cos\alpha$. These were used to calculate ω for $d\cos\alpha = 0.1$, 1 and 10 and C_3 and C_4 for $d\cos\alpha = 1$. The values of C_3 and C_4 calculated here are presented in Table I (C_3 and C_4 for the two limiting cases are presented in Mullins' original paper). The calculations for ω are presented in Figure 15. The facet profile for $d\cos\alpha = 1$ was calculated from equation (7) for

Table I

The Constants C_3 and C_4 as Functions of ω for $d \cos \alpha = 1$

ω	C_3	C_4
0	1.000	-9.402×10^{-2}
0.2	1.009	-9.676×10^{-2}
0.4	1.032	-1.025×10^{-1}
0.6	1.052	-1.124×10^{-1}
0.8	1.081	-1.262×10^{-1}
1.0	1.096	-1.439×10^{-1}
1.2	1.084	-1.663×10^{-1}
1.4	1.040	-1.925×10^{-1}
1.6	9.508×10^{-1}	-2.232×10^{-1}
1.8	8.047×10^{-1}	-2.591×10^{-1}
2.0	5.574×10^{-1}	-2.981×10^{-1}
2.2	2.208×10^{-1}	-3.394×10^{-1}
2.4	-2.421×10^{-1}	-3.832×10^{-1}
2.6	-8.676×10^{-1}	-4.270×10^{-1}
2.8	-1.644	-4.637×10^{-1}
3.0	-2.618	-4.978×10^{-1}
3.2	-3.800	-5.143×10^{-1}
3.4	-5.176	-5.221×10^{-1}
3.6	-6.800	-5.019×10^{-1}
3.8	-8.563	-4.471×10^{-1}
4.0	-1.048×10	-3.577×10^{-1}
4.2	-1.250×10	-2.165×10^{-1}
4.4	-1.447×10	-2.139×10^{-2}
4.6	-1.627×10	2.431×10^{-1}
4.8	-1.778×10	5.701×10^{-1}
5.0	-1.888×10	9.822×10^{-1}

$m/n = 1.04$ and is presented in Figure 16, where it is compared to the profiles calculated by Mullins for $d \cos \alpha = 0$ and $d \cos \alpha = \infty$.

An important conclusion from the present calculations is this: for small m/n it is difficult to distinguish between the cases $d \cos \alpha = 1$ and $d \cos \alpha = \infty$. In Figure 15 it can be seen that the curve for $d \cos \alpha = 1$ falls quite near the $d \cos \alpha = \infty$ curve for small m/n. Similarly the $d \cos \alpha = 1$ profile in Figure 14 is very near the $d \cos \alpha = \infty$ profile. Mullins obtained expressions for m/n as a function of ω for the two limiting cases by expanding his equation number (21)*:

$$\frac{m}{n} = 0.6409\,\omega + 0.09745\,\omega^2 - 0.002422\,\omega^3 \qquad (8a)$$

$$\underline{d \cos \alpha = \infty}$$

$$\frac{m}{n} = 1.281\,\omega + 0.459\,\omega^2 + 0.0588\,\omega^3 \qquad (8b)$$

$$\underline{d \cos \alpha = 0}$$

If Mullins' equation (21) is expanded as a series for the general case, it gives the form

$$\frac{m}{n} = (a_1\omega + a_2\omega^2 + a_3\omega^3 + \cdots\cdots) + \left(\frac{\omega}{d \cos \alpha}\right)(b_1\omega + b_2\omega^2 + b_3\omega^3 + \cdots\cdots) + \left(\frac{\omega}{d \cos \alpha}\right)^2 (c_1\omega + c_2\omega^2 + c_3\omega^3 + \cdots\cdots) + \cdots\cdots \qquad (9)$$

* In Mullins's paper[2], equations (8) were given incorrectly; the correct forms are given here[36].

The constants a_1, a_2 and a_3 are the same as those of equation (8a). From the form of equation (9) and the values of the a's, it can be seen that for d cos $\alpha \neq 0$ and small ω, m/n will be very close to the curve of Figure 15 for d cos $\alpha = \infty$; this is apparent for the d cos $\alpha = 1$ curve for $m/n \leq 1.5$ and for the d cos $\alpha = 10$ curve for $m/n \leq 3$. Equation (9) can be rewritten in a slightly different form to obtain equation (8b) as d cos α approaches zero. However, for d cos $\alpha \neq 0$, the correct limiting behavior for small ω is given by equation (8a).

Three of the observed facet profiles are shown in Figure 16. These were determined by tracing along a given fringe on a print such as Figure 10, measuring the fringe height as a function of distance from the facet center and then multiplying by the appropriate numbers to give the facet the standard slope and size. Almost all of the separated facets observed had m/n less than unity. It was noted earlier that, for orientations quite near (111), where m/n would be larger than one, facets nucleated very easily so that many small closely spaced facets formed rather than large separated facets. Hence, the curved surface profiles were observable only for m/n less than about unity.

Comparison of Figures 15 and 14 shows that the observed profiles fall between the curves calculated for the two limiting cases d cos $\alpha = 0$ and d cos $\alpha = \infty$. It is tempting to conclude from this that D_s and D_c do not differ by more than a factor of about ten. However, this conclusion assumes that surface diffusion is the mechanism of facet formation. The considerations of the previous section cast some doubt on this assumption. If volume diffusion is for some reason the dominant

transport mechanism, then transport through the volume under (or over) the low index flat will occur with the same D as under (or over) the curve region on either side. Thus this would fit the contour in which $D_s \simeq D_c$.

Rhead[19] has measured the profiles of separated facets on silver and has calculated ω as a function of m/n for several of these facets. He observed that his points fall quite close to the d cos $\alpha = \infty$ curve, but they appear to lie just as close to the d cos $\alpha = 1$ curve. Rhead measured the rate of grain boundary grooving on his faceted specimens and from this concluded that in his case most of the matter was transported by surface diffusion. Hence the comparison of the calculated and observed profiles seems to be valid in his case, and it can be concluded that, at least for silver in air, D_s does not appear to be greatly different from D_c.

In conclusion of this section, it must be noted that, for experimentally observable cases ($m/n < 1$), it is difficult to distinguish between d cos $\alpha = 1$ and d cos $\alpha = \infty$. From the available experimental evidence, it appears that, assuming surface diffusion is the mechanism of facet formation, the surface diffusion coefficients are roughly the same on the simple surface and on the complex surface. This agrees with the results of Choi and Shewmon[33,34] who found that the surface diffusion coefficient varied by not more than a factor of three over the entire unit triangle. However, the copper surfaces in these experiments were covered with about a half monolayer of oxygen[5], while the surfaces of Choi and Shewmon were free of oxygen. As Blakely has pointed out in

his recent review[37], impurity adsorption could either accelerate or retard surface diffusion. There exists, so far, very little evidence as to how adsorption affects surface diffusion.

Concluding Discussion

The evidence of section 3 of the Results indicates that volume diffusion within the crystal can account for the observed facets. On the other hand, in section 4 of the Results it was shown that the observed facet profiles agree reasonably well with the profiles predicted by Mullins' analysis[2], with D_s/D_c near unity. It must be pointed out that neither in this work nor in the work of Rhead[19] have the kinetics of facet formation been studied by actually observing the growth of individual facets. It was attempted to follow the growth of individual facets by annealing, cooling, examining, and then reannealing, but this was unsuccessful. During the cooling and reheating, additional facets nucleated near the original facets, impeding their growth. In some cases, the facets appeared to stop growing or even to diminish in size on reannealing. Rhead[19] reports similar difficulties in observing the growth of individual facets, as does Moore[38]. It would be desirable to devise a method for actually observing the growth of particular facets, so that the mechanism could be determined exactly. Since it has been shown that it is possible to produce separated facets, it appears that the kinetics of facet formation could be elucidated more clearly by further work.

From this work it is seen that knowledge of the τ/γ vs θ curve under the conditions of facet formation is helpful in deciding whether or not the facets are thermodynamically stable. If they are stable, the τ/γ vs θ curve can indicate at which orientations it will be difficult to nucleate facets, so that in this region separated facets for the study of the kinetics of faceting can be produced. From the present results it is seen that facets are stable for a range of orientations near (111) and separated facets are produced in the range of orientations ten to twenty degrees from (111).

Acknowledgments

The interest and encouragement of Professor P. G. Shewmon in carrying out this work is greatly appreciated. The author would like to acknowledge many discussions with Dr. A. J. W. Moore. The grant of a Graduate Fellowship and a Postdoctoral Fellowship by the National Science Foundation for the period over which this work was done is gratefully acknowledged. This work was also supported by the Office of Naval Research under contract number Nonr-760(19).

REFERENCES

1. A. J. W. Moore, "Thermal Faceting," ASM-AIME Seminar on Surfaces: Structure, Energetics and Kinetics, New York, Oct. 27-28, 1962.

2. W. W. Mullins, "Theory of Linear Facet Growth during Thermal Etching," Phil. Mag. 6, 1313 (1961).

3. W. W. Mullins and P. G. Shewmon, "The Kinetics of Grain Boundary Grooving in Copper," Acta Met. 7, 163 (1959).

4. C. S. Barrett, Structure of Metals, McGraw-Hill Book Co., (New York, 1952), p. 194.

5. W. M. Robertson and P. G. Shewmon, "Crystallography of Impurity Adsorption on Copper Surfaces," J. Chem. Phys. (to be published).

6. W. M. Robertson and P. G. Shewmon, "Variation of Surface Tension with Surface Orientation in Copper," Trans. AIME, 224, 804 (1962).

7. J. Bénard, J. Moreau and F. Gronlund, "Nouvelles Observations sur le Rule de l'Oxygene Adsorbe dans le Modifications du Profil d'Equilibre des Surfaces Metalliques aux Temperatures Elevees," Comptes Rendus 246, 756 (1958).

8. A. J. W. Moore, "The Influence of Surface Energy on Thermal Etching," Acta Met. 6, 293 (1958).

9. J. Moreau and J. Bénard, "Influence de l'Orientation Cristalline sur l'Edification du Profil d'Equilibre de Surfaces de Cuivre et d'Argent par Traitement Oxydant aux Temperatures Elevees," Comptes Rendus 248, 1658 (1958).

10. C. G. Dunn and J. L. Walter, "Discussion of 'Experimental Evidence of Boundary Migration,'" Acta Met. 8, 60 (1960).

11. B. Chalmers, R. King and R. Shuttleworth, "The Thermal Etching of Silver," Proc. Roy. Soc. A193, 465 (1948).

12. J. Bénard, "Equilibres Chimiques Reversibles a la Surface Solides," Bull. Soc. Chim. France 27, 203 (1960).

13. J. Moreau, "Influence de l'Orientation Cristalline de la Surface d'Alliage Fer-Chrome sur la Formation du Profil d'Equilibre aux Temperatures Elevees," Comptes Rendus, 246, 2476 (1958).

14. J. Moreau and J. Bénard, "Sur la Striation Reversible du Fer et de Ses Alliages," Acta Met. 10, 247 (1962).

15. J. Oudar, F. Brouty, and J. Bénard, "Striation Reversible des Surfaces Metalliques dans les Atmospheres Faibiement Sulfurantes," Acta Met. 9, 520 (1961).

16. F. Cabane-Brouty, J. Oudar and J. Bénard, "Etude Quantitative des Equilibres Reversibles de Striation de l'Argent dans les Atmospheres Faiblement Sulfurantes," Acta Met. 10, 901 (1962).

17. G. E. Rhead and H. Mykura, "Thermal Etching of Silver," Acta Met. 10, 578 (1962).

18. G. E. Rhead and H. Mykura, "Thermal Etching of Silver in Various Atmospheres," Acta Met. 10, 843 (1962).

19. G. E. Rhead, "Surface Self-Diffusion and Faceting on Silver," (to be published).

20. E. C. Hondros and A. J. W. Moore, "Evaporation and Thermal Etching," Acta Met. 8, 647 (1960).

21. A. J. W. Moore, "Reply to a Letter on 'Thermal Etching of Silver,'" Acta Met., 10, 579 (1962).

22. C. Herring, "Some Theorems on the Free Energies of Crystal Surfaces," Phys. Rev. 82, 87 (1951).

23. C. Herring, "The Use of Classical Macroscopic Concepts in Surface Energy Problems," Chapter in Structure and Properties of Solid Surfaces, ed. by R. Gomer and C. S. Smith (University of Chicago, 1953).

24. E. Gruber, Carnegie Institute of Technology, Private communication.

25. C. Herring, "Surface Tension as a Motivation for Sintering," Chapter in The Physics of Powder Metallurgy, ed. by W. E. Kingston, (McGraw-Hill Book Co., New York, 1951).

26. H. Mykura, "Twin Boundary Free Energies and the Variation of Surface Free Energies with Crystallographic Orientation," Acta Met. 5, 346 (1957).

27. H. Mykura, "The Variation of Surface Tension of Nickel with Crystallographic Orientation," Acta Met. 9, 570 (1961).

28. N. A. Gjostein, "Adsorption and Surface Energy (II): Thermal Faceting from Minimization of Surface Energy," Acta Met. (to be published).

29. N. A. Gjostein, "On the Orientation Dependence of Surface Free Energy," Acta Met. 7, 812 (1959).

30. P. G. Shewmon and W. M. Robertson, "Variation of Surface Tension with Orientation," ASM-AIME Conference on Surfaces: Structure, Energetics

and Kinetics, New York, Oct. 27-28, 1962.

31. R. B. McLellan and R. Shuttleworth, "The Vapor Pressure of Solid Copper," Zeit. Metallkunde 51, 149 (1960).

32. N. A. Gjostein, "Measurement of the Surface Self-Diffusion Coefficient of Copper by the Thermal Grooving Technique," Trans. AIME 221, 1039 (1961).

33. J. Y. Choi and P. G. Shewmon, "Effect of Orientation on the Surface Self-Diffusion of Copper," Trans. AIME 224, 589 (1962).

34. P. G. Shewmon and J. Y. Choi, "Anisotropy of the Surface Diffusion Coefficients for Copper," Trans. AIME 227, 515 (1963).

35. W. W. Mullins, "Grain Boundary Grooving by Volume Diffusion," Trans. AIME 218, 354 (1960).

36. W. W. Mullins, private communication.

37. J. M. Blakely, "Surface Diffusion," Progress in Material Science 10, p. 395 (Pergamon Press, 1963).

38. A. J. W. Moore, private communication.

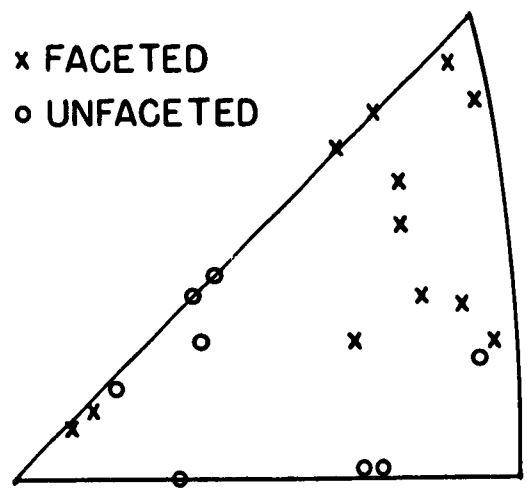

Figure 1. Faceting as a function of surface orientation for $\ell n\ p_{H_2O}/p_{H_2} = -3.5$. Faceted surfaces (x); unfaceted surfaces (o).

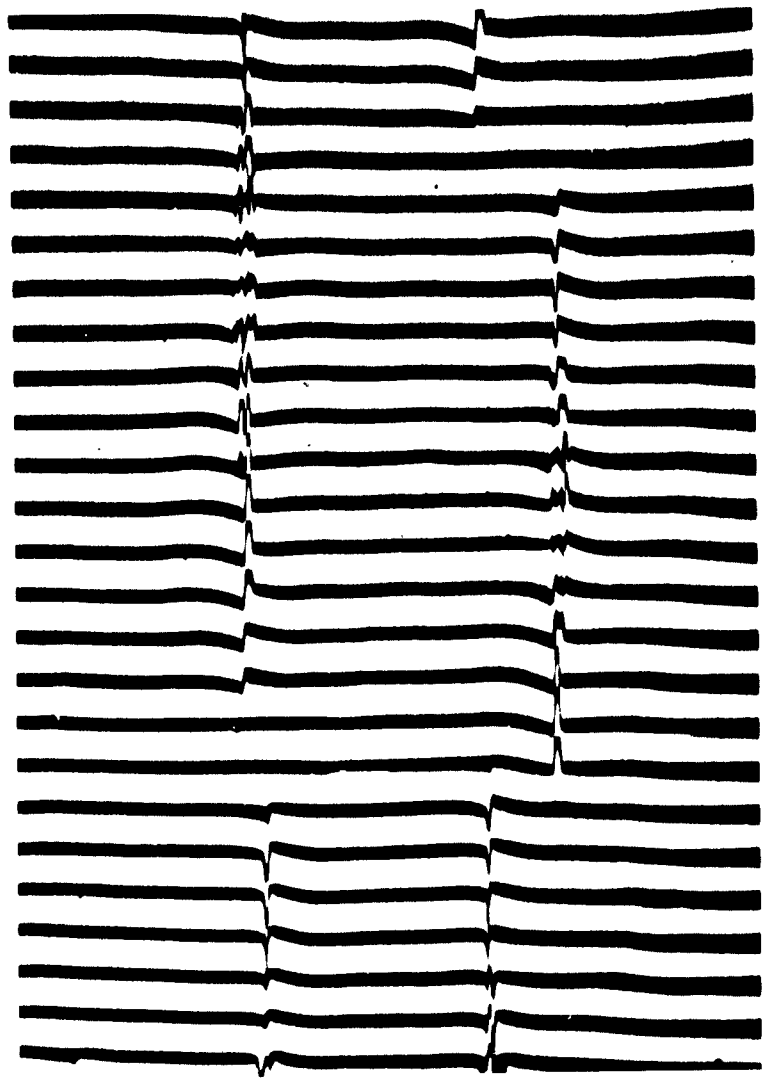

Figure 2. Surface of sample about 20° from (100), showing both (100) and (111) facets. X865; fringe spacing = 0.27 μ.

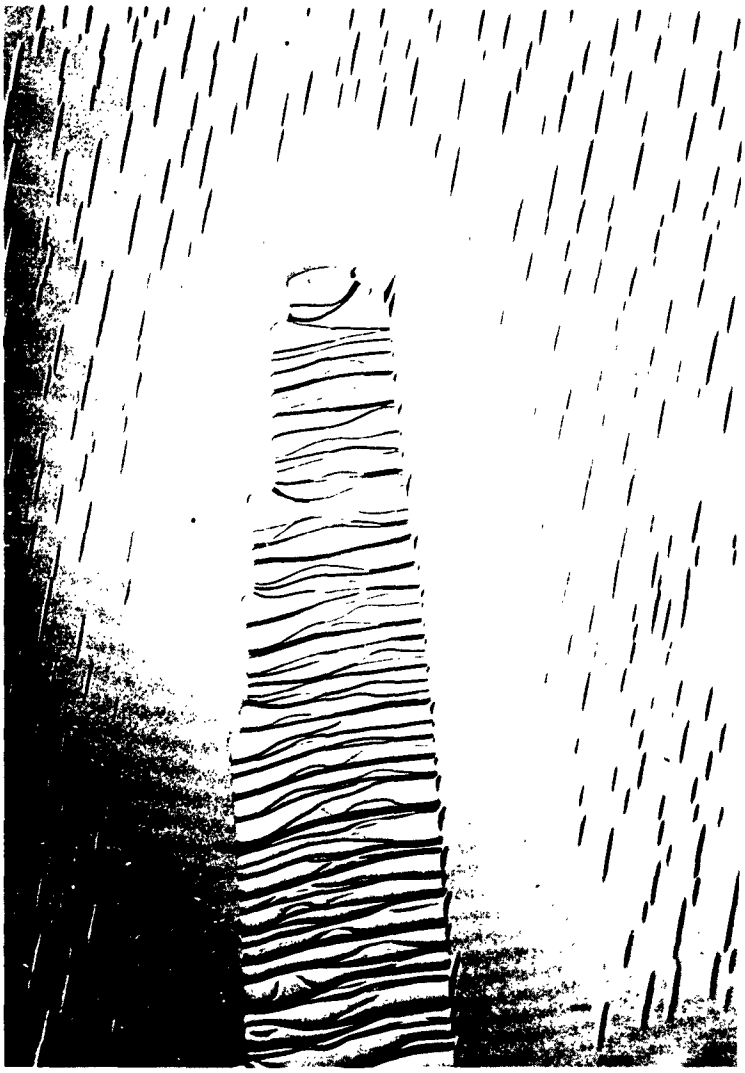

Figure 3. Light faceting on one grain that seems to be inhibited near an adjacent heavily faceted grain. X730.

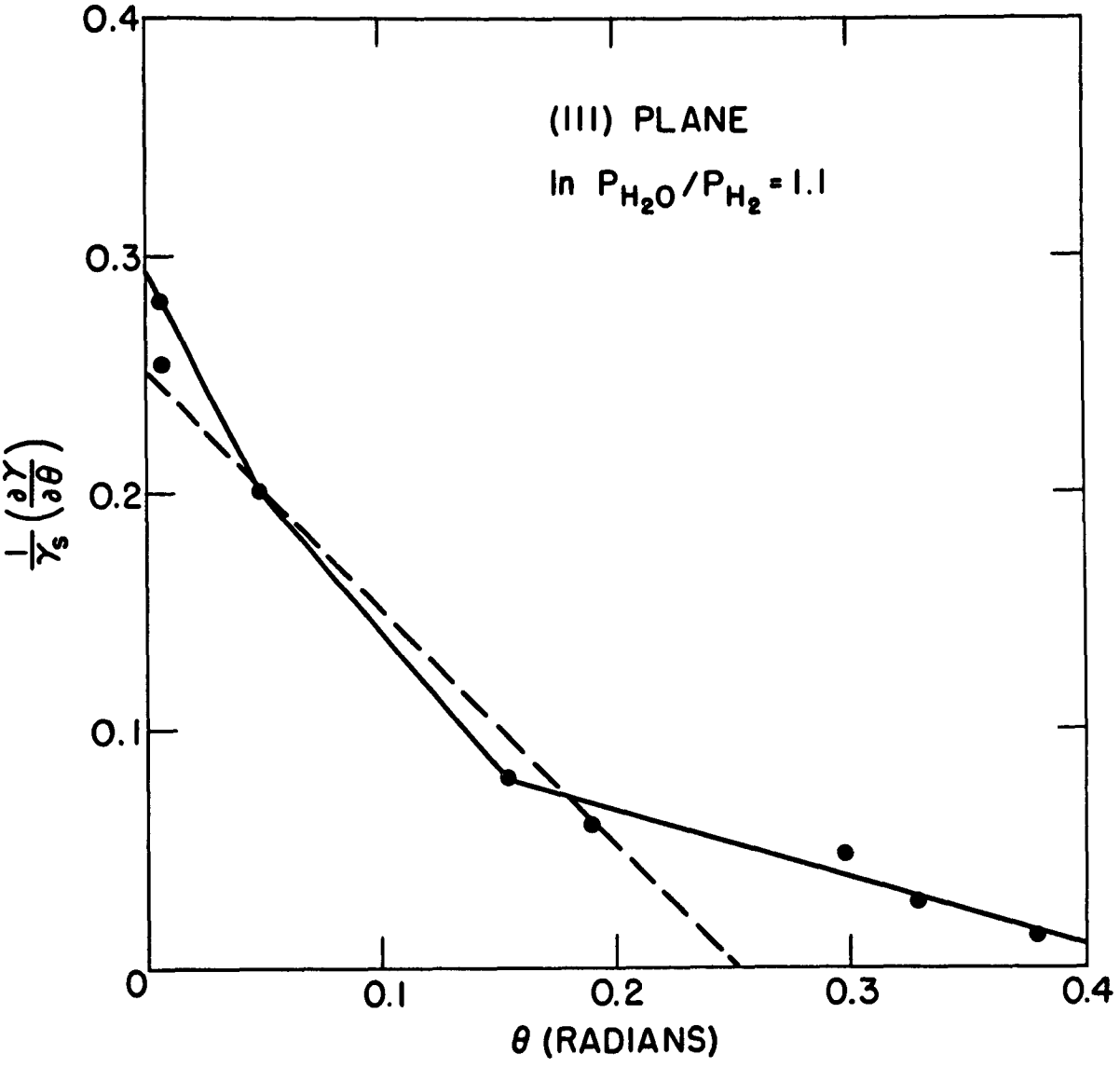

Figure 4. Plot of τ/γ as a function of θ for surfaces near (111) for $\ell n\ p_{H_2O}/p_{H_2} = 1.1$.

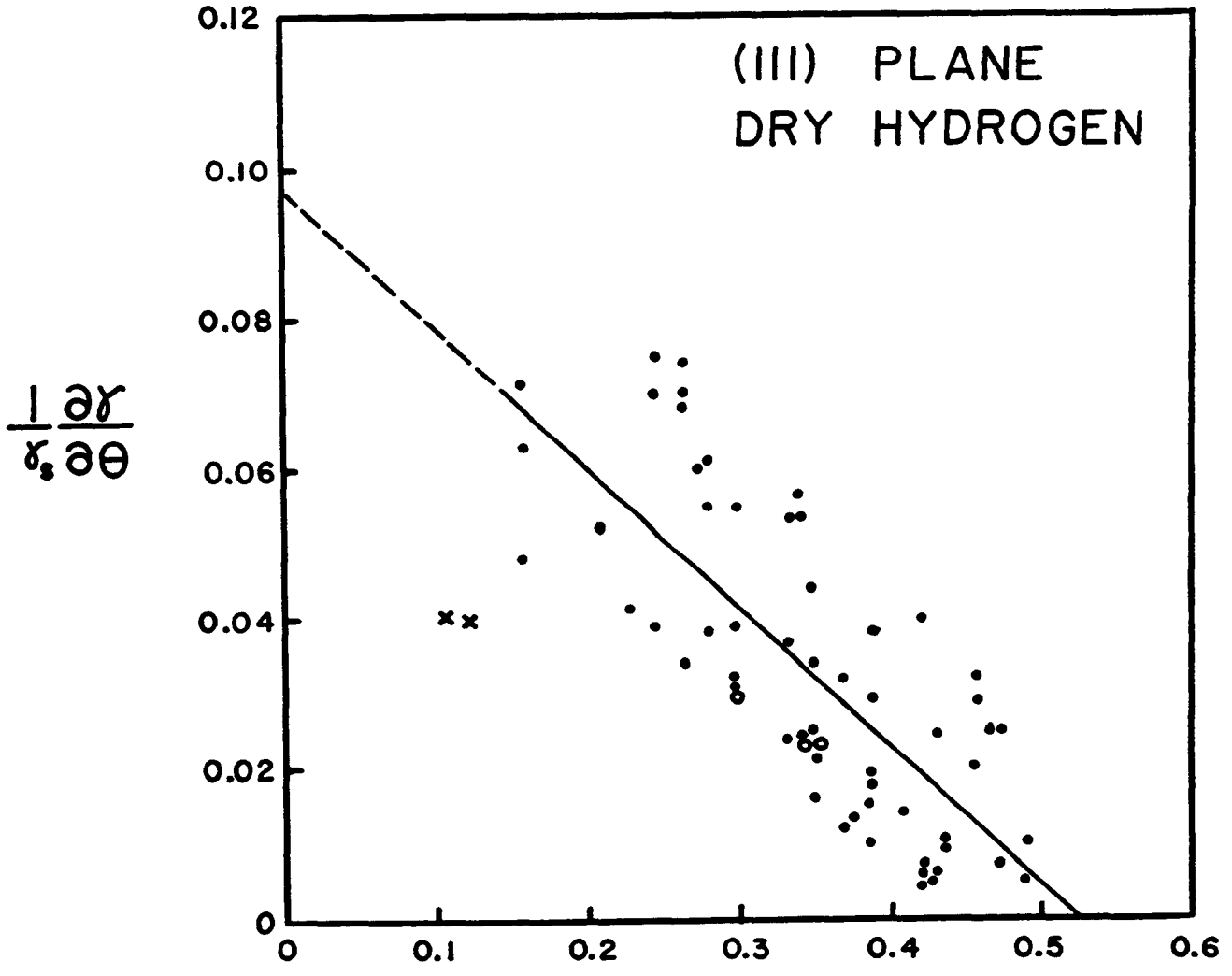

Figure 5. Plot of τ/γ as a function of θ for surfaces near (111) for $\ell n\ p_{H_2O}/p_{H_2} = -9.5$ (from Ref. 6).

•: OFHC copper in graphite boat; o: high purity copper in graphite boat; x:OFHC copper with no graphite.

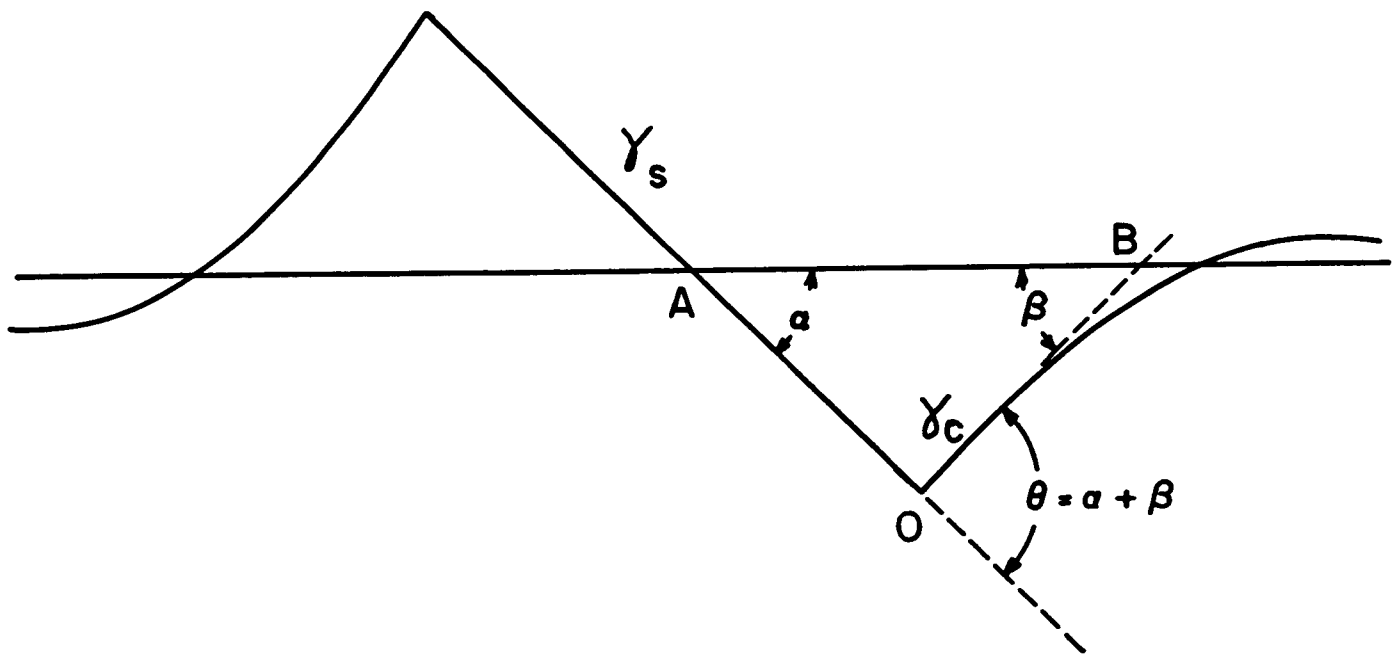

Figure 6. Surface profile of a facet (schematic), showing the equilibrium edge angles.

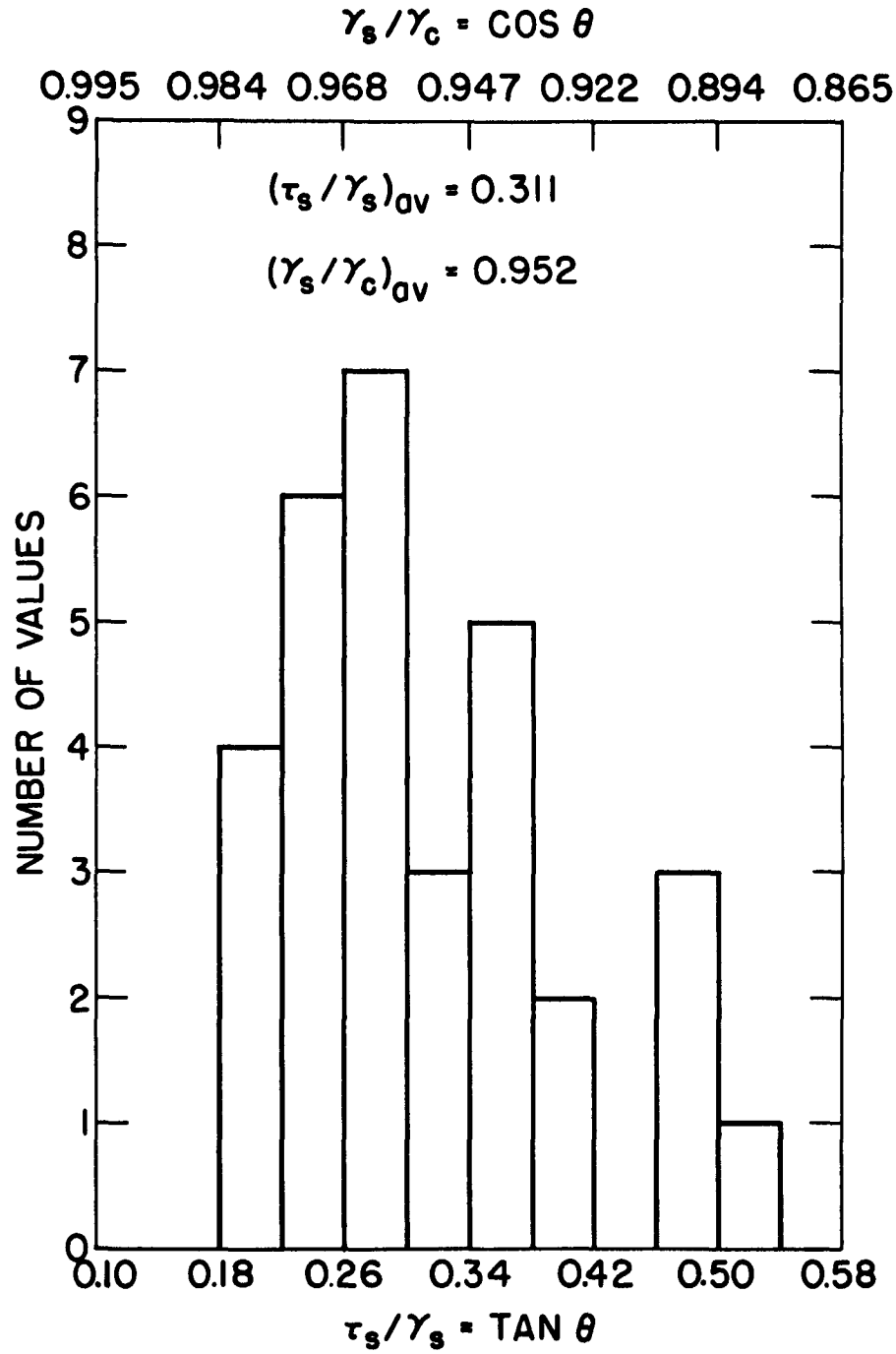

Figure 7. Plot of the frequency of occurrence of different values of τ_s/γ_s and γ_s/γ_c as determined from facet edge angles.

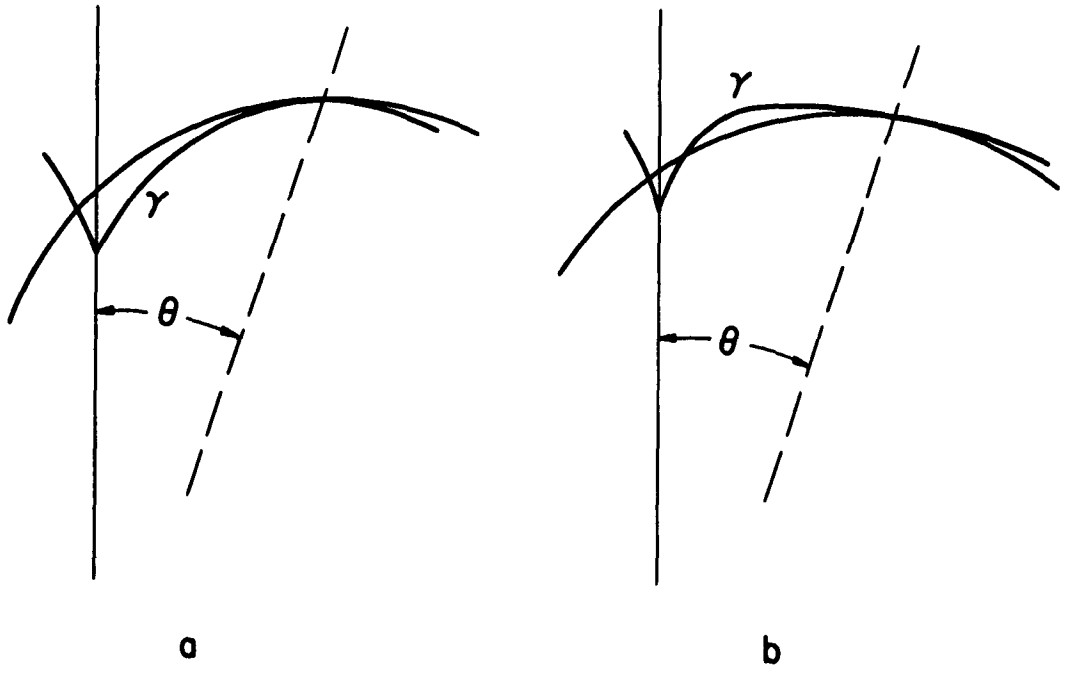

Figure 8. Schematic two-dimensional γ-plots for faceting conditions with a sphere tangent at orientation θ.
(a) No nucleation barrier to faceting;
(b) Nucleation barrier to faceting exists.

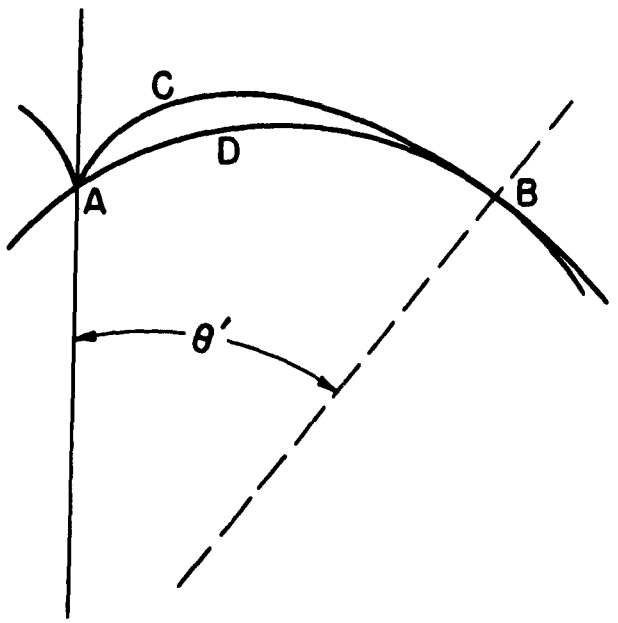

Figure 9. Schematic γ-plot ACB showing sphere ADB tangent at θ', the limit of faceting.

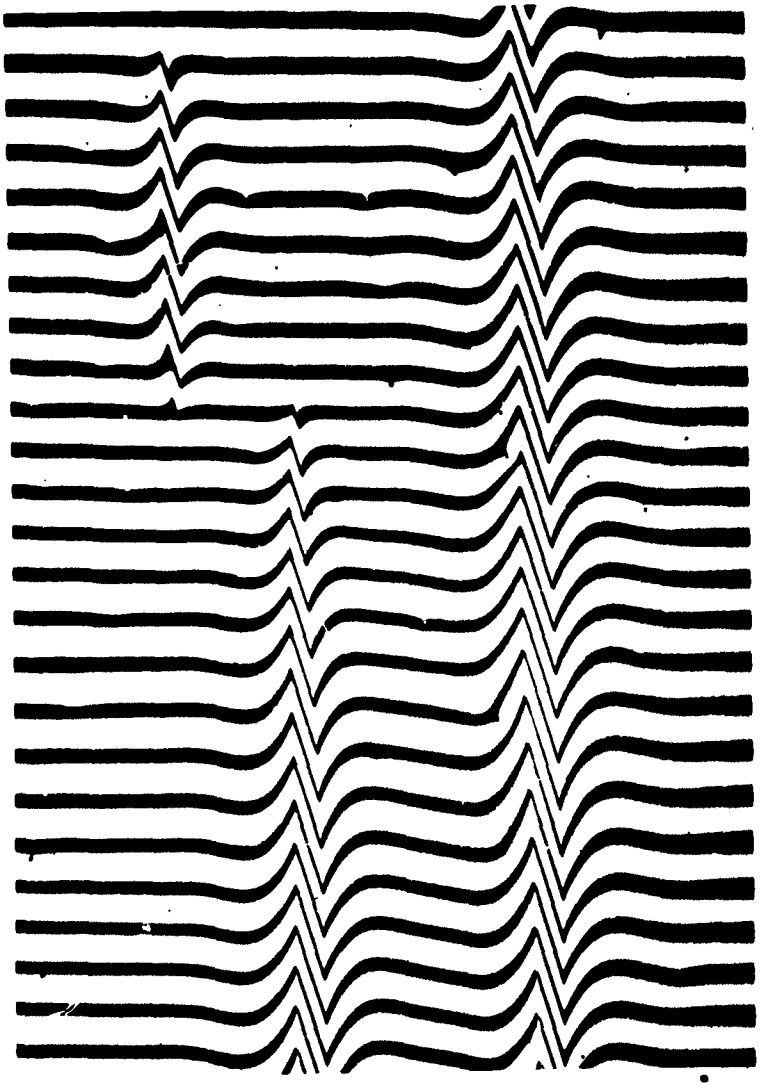

Figure 10. Separated facets showing the contours of the curved, high index surface. X865; fringe spacing = 0.27 μ.

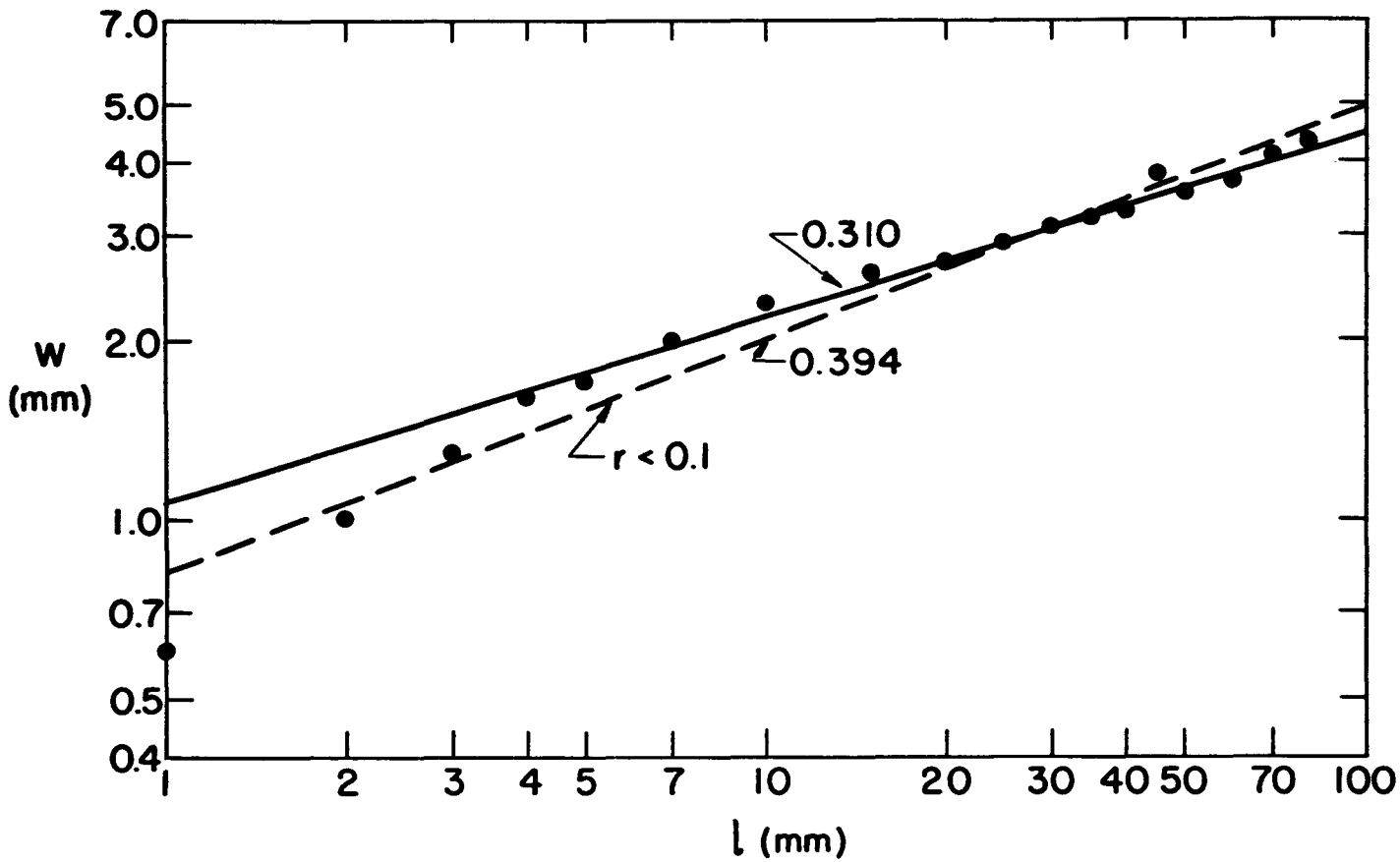

Figure 11. Logarithmic plot of width ω of a lens-shaped facet versus distance ℓ from facet end. ω and ℓ in millimeters, measured on a point at X865.

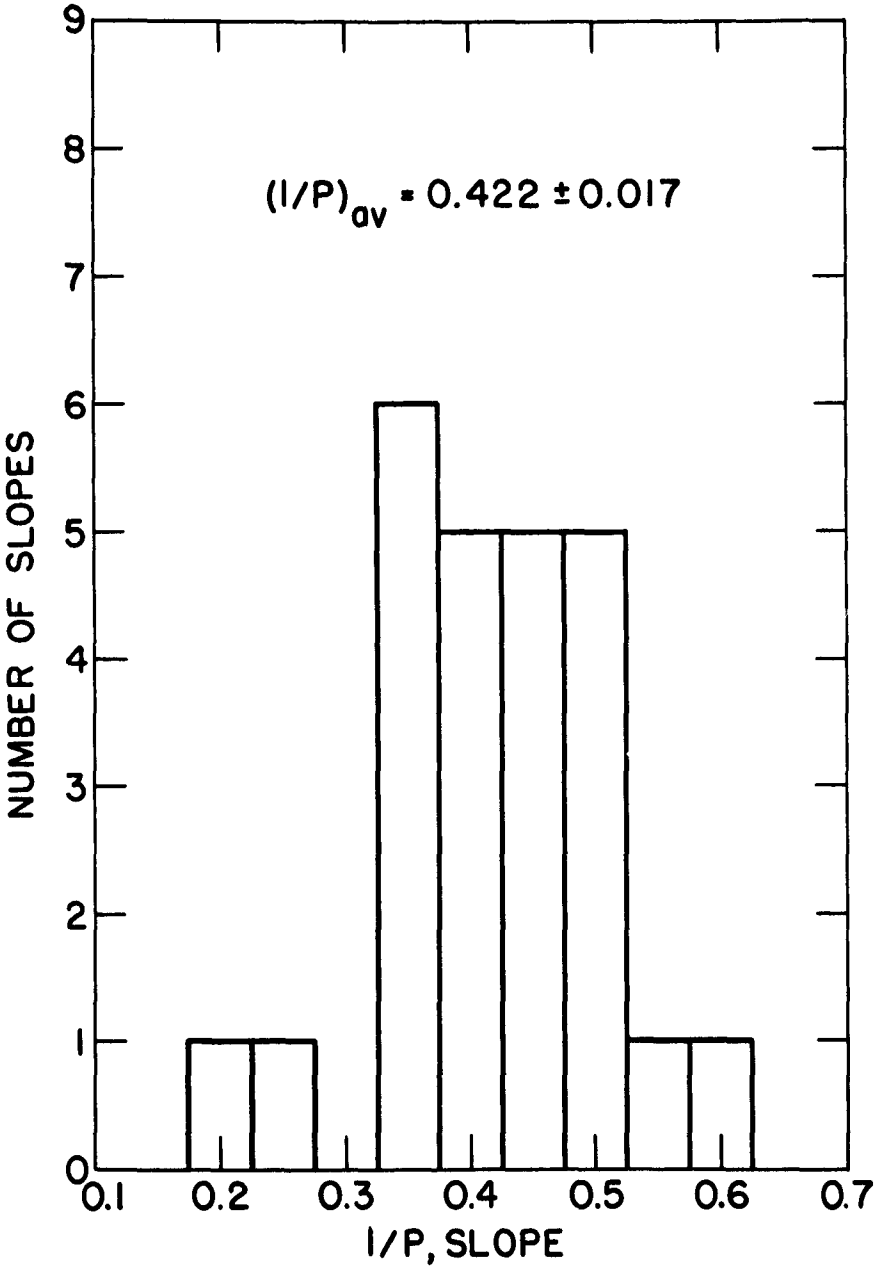

Figure 12. Frequency of occurrence of slopes of log ω versus log ℓ plots similar to Figure 11.

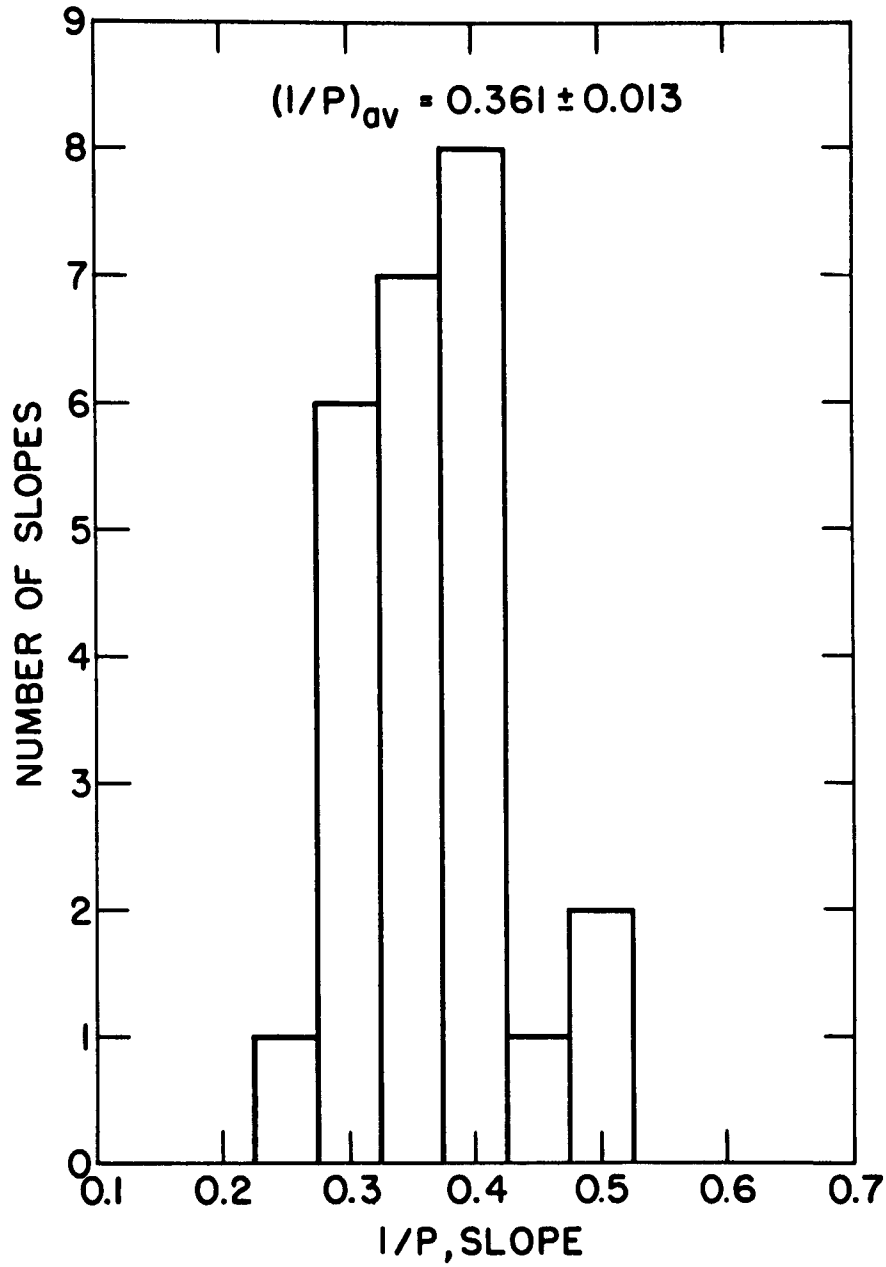

Figure 13. Frequency of occurrence of slopes of log ω versus log ℓ plots, neglecting points for ℓ < 5 mm.

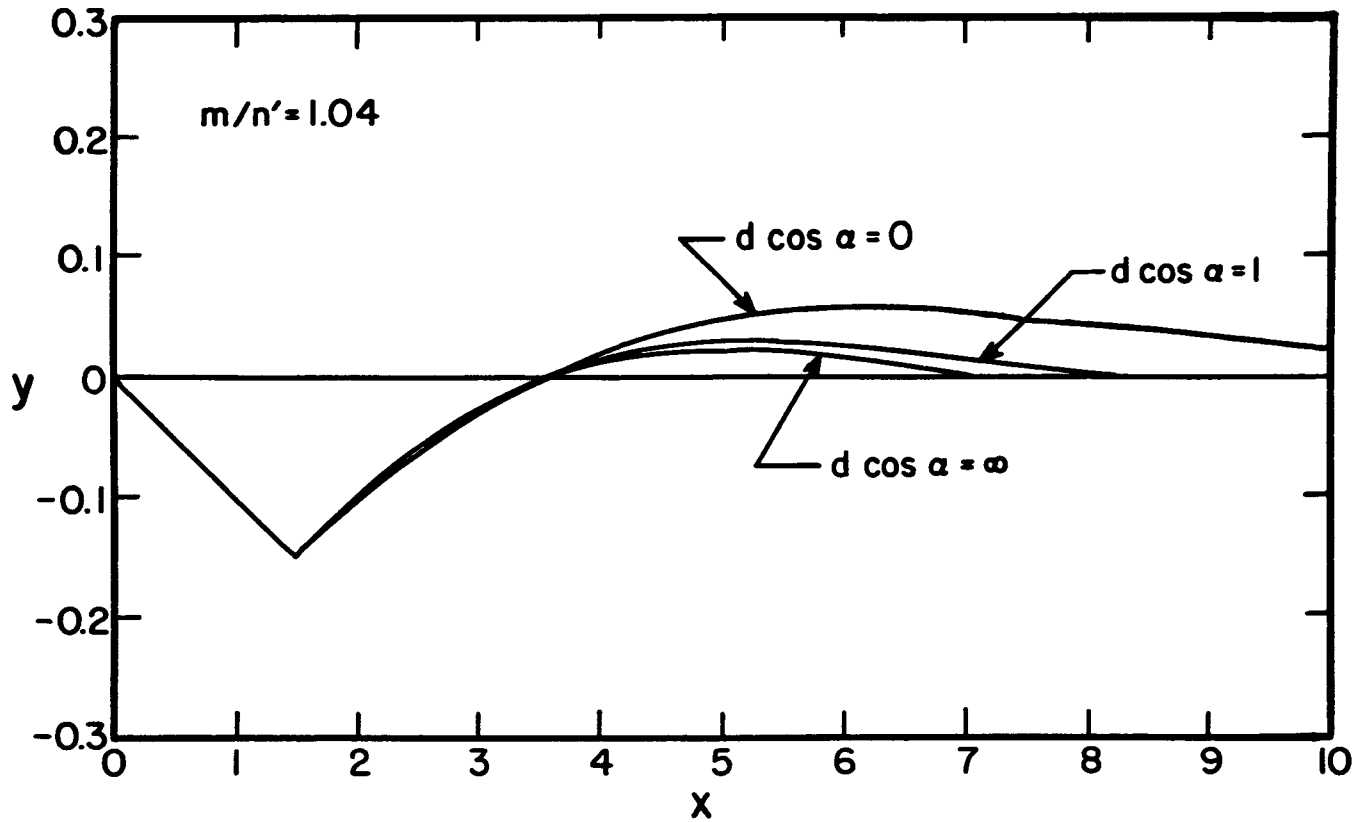

Figure 14. Calculated standardized profiles of separated facets for m/n = 1.04 for various values of d cos α. Curves d cos α = 0 and d cos α = ∞ from Mullins[2]; curve d cos α = 1, this work.

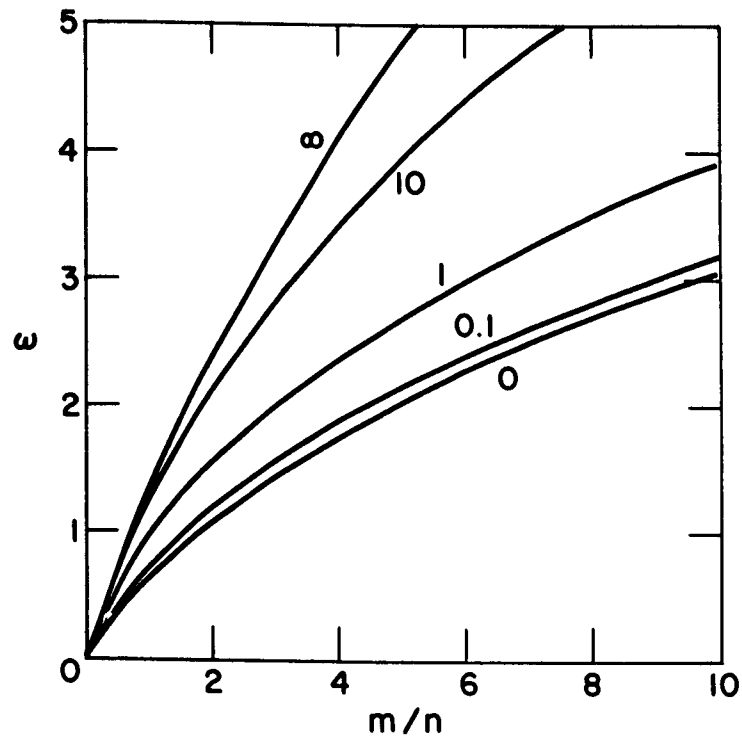

Figure 15. Plot of ω as a function of m/n. Attached numbers give values of d cos α. Curves d cos α = 0 and d cos α = ∞ from Mullins[2].

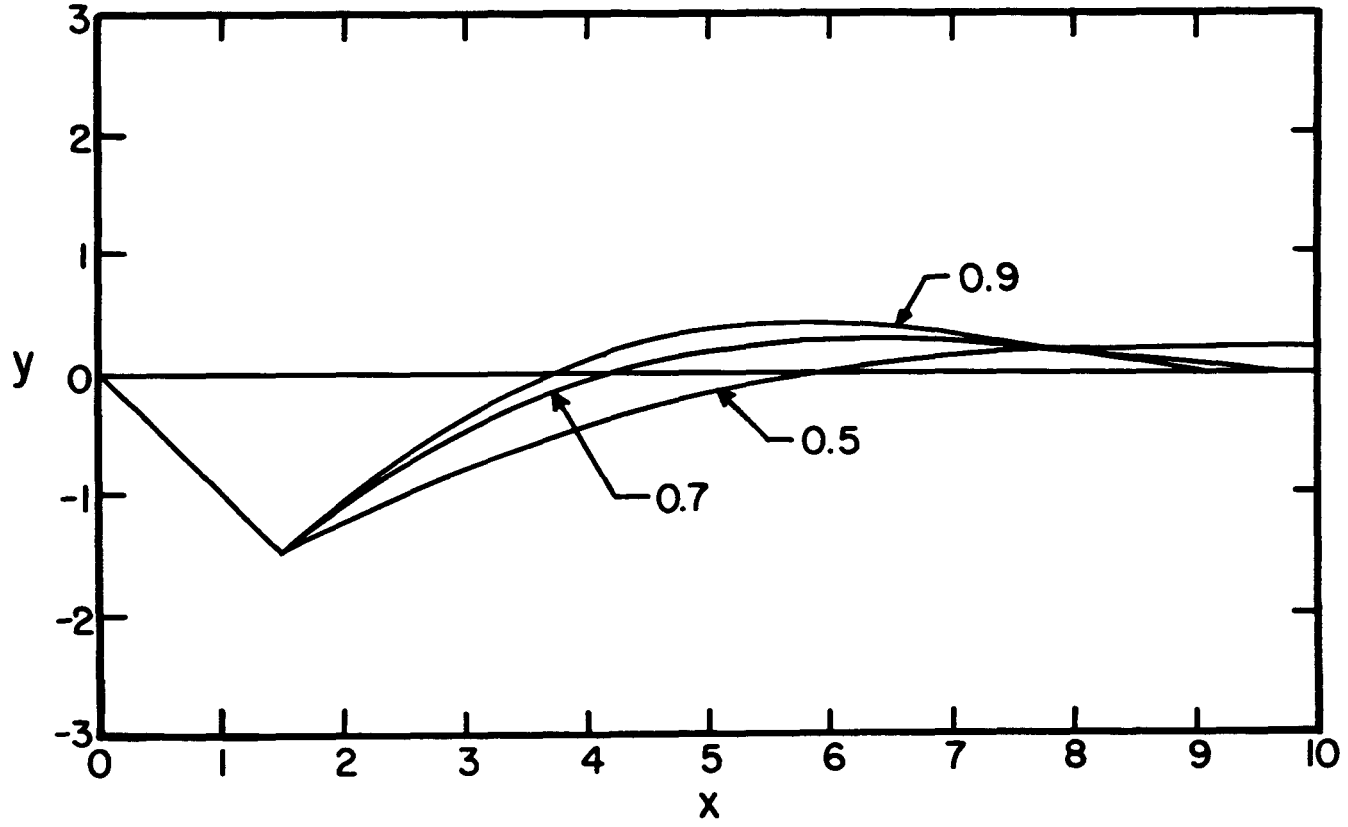

Figure 16. Standardized profiles of observed separated facets. Attached numbers give values of $m/n \equiv \tan \beta/(-\tan \alpha)$.